

Effect of surface preparation on adhesive bonding of CFRP compression molding laminates

Siciliani Vincenzina^{1,a*}, Pelaccia Riccardo^{1,b}, Alfano Marco^{1,c}, Castagnetti Davide^{1,d}, Raimondi Luca^{2,e}, Zanchi Alessandro^{2,f}, Donati Lorenzo^{2,g}, and Orazi Leonardo^{1,h}

¹DISMI – University of Modena and Reggio Emilia, via Amendola 2, 42122 Reggio Emilia, Italy

²DIN – Department of Industrial Engineering, Alma Mater Studiorum Università di Bologna, Viale Risorgimento 2, Bologna, 40136, Italy

³EN&TECH – University of Modena and Reggio Emilia, Piazzale Europa 1, 42124 Reggio Emilia, Italy

^{a*}vincenzina.siciliani@unimore.it, ^briccardo.pelaccia@unimore.it, ^cmarco.alfano@unimore.it, ^ddavide.castagnetti@unimore.it, ^eluca.raimondi@unibo.it, ^falessandro.zanchi5@studio.unibo.it, ^gl.donati@unibo.it, ^hleonardo.orazi@unimore.it,

(*corresponding author)

Keywords: laser texturing, adhesive bonding, shear strength.

Abstract. Composite structures are increasingly being used across various industries to promote structural lightweighting but also because of their excellent fatigue and corrosion resistance. To further minimize weight while preserving these benefits, adhesive bonding is now widely used to join advanced composite materials. However, effective surface pretreatments are essential to ensure suitable joint mechanical properties, including strength, fracture toughness, and long-term durability. The present study investigates viable surface preparation methods for a carbon fiber reinforced composite obtained through compression molding. Both standard mechanical abrasion and advanced ultrashort UV-laser treatment were evaluated. The effect of surface modification on surface morphology was evaluated using Scanning Electron Microscopy (SEM), while the corresponding modification of surface chemistry was determined using Energy Dispersive X-ray Spectroscopy (EDS). The combined results allowed us to judge the ability of the proposed strategies to modify surface morphology and remove post-processing contamination, primarily silicon-based. Besides, displacement-controlled tensile tests were conducted on adhesive-bonded single-lap joints to assess joint strength. The results show that UV laser ablation effectively removes contaminants on the matrix material without damaging the carbon fibers, improving adhesive joint shear strength compared to sanded specimens.

Introduction

Several industries, particularly automotive, aerospace, and defense, are actively pursuing lightweight designs by assembling multi-material or composite structures. Among them, carbon fiber-reinforced polymer (CFRP) composites are widely used because of their excellent fatigue resistance and electrochemical properties, as well as low weight. [1,2]

The joining of composite materials presents significant challenges due to their heterogeneous material properties. Thermosetting polymers, for example, are incompatible with conventional welding techniques, while both thermosets and thermoplastics pose difficulties for traditional mechanical fastening methods, such as riveting. These challenges arise from factors such as stress concentrations and the potential for material damage during the fastening process [2]. Bonding



using structural adhesives can offer several advantages with respect to traditional fastening methods, such as good strength, vibration damping, corrosion resistance, uniform stress distribution, and design flexibility. It is also unavoidable to join large-scale composite parts [3]. Secondary bonding of two CFRP parts, which represents the joining of two cured parts using a structural adhesive that is subsequently cured, is versatile, easy to handle and to integrate into the manufacturing process.

The bonding of composite materials can be challenging due to the presence of mold release agents, which serve as contaminants, often in the form of monolayer adsorbates on the surface. Silicon is considered one of the most harmful contaminants, as it can significantly impair adhesive bonding and negatively affect the overall performance of the joint. Furthermore, during processes such as compression molding, there is potential for silicon to migrate slightly into the near-surface region of the matrix. As a result, thorough surface preparation is crucial prior to bonding to address these issues and ensure optimal joint performance [4].

Besides, effective surface pretreatments are required to increase joint strength and fracture toughness, since these are affected by surface morphology, topography, interface composition, and mechanical performance of the adherend-adhesive interface [2].

Common pretreatment methods, such as mechanical abrasion (sanding), are used to remove contaminants, increase surface energy, and improve adhesive-substrate contact. However, sanding can be labour-intensive, particularly for large structures, and often results in a non-uniform surface finish. It also involves a trade-off between effective contaminant removal and the potential damage to surface fibers. Laser treatments may enable selective removal of the composite matrix while preserving the integrity of the reinforcing fibers and ensuring robust, repeatable, and reliable processes [12]. Different laser treatment types have been employed to treat thermoset composites, aiming at removing contaminants from the adherend, or surface texturing to modify surface roughness, morphology, and chemistry or to uncover surface fibers and promote toughening through fiber bridging [5–9].

Laser irradiation can simultaneously modify surface chemistry and morphology, improving physicochemical bonding mechanisms and mechanical interlocking, thereby increasing the adhesive bond strength and/or fracture toughness compared with untreated specimens [10–12].

UV lasers are mainly used to remove silicon contaminants of the release agent from processes that use molds for manufacturing. Short wavelength laser light is typically used to treat temperature-sensitive materials, such as polymeric-based matrix, since it has a less pronounced photo-thermal effect on the polymer. Specific surface cleaning treatments are made possible by laser treatment, which facilitates adhesion control [2].

In this study, both sanding and UV picosecond laser treatment are employed for the surface preparation of CFRP adherends. Surface morphology of the untreated, sanded, and laser-treated specimens is characterized using scanning electron microscopy (SEM), while the presence of silicon compounds is quantitatively assessed via energy dispersive spectroscopy (EDS). The interactions between the laser and CFRP are examined, revealing significant variations in surface topography and morphology. Finally, single-lap adhesive joints with sanded and laser-treated surfaces are fabricated for mechanical testing to evaluate shear strength and the corresponding failure mechanisms.

Materials and Methods

Substrate and adhesive materials

An automotive grade prepreg, designated as SC160/RC200P, was supplied by Gurit (Newport, UK) to produce the composite substrates used in this study. This material features a 2×2 twill weave fabric made from Toray T300 carbon fibers. It has a nominal areal weight of 195 g/m^2 , a tow size of 3K, and is impregnated with 40% by weight of Gurit SC160 epoxy resin. The prepreg was extracted from cold storage for 5h before being cut and put in a white chamber. To prevent defect formation during processing [13], square preforms of $320 \times 320 \text{ mm}$ were extracted from the roll in the 0° direction and hand laid up with a staking sequence of $[0^\circ/90^\circ]_6$. Prepreg compression molding was performed into a specifically designed mold featuring a $320 \times 320 \text{ mm}$ cavity and installed into an industrial downstroke AEM3 press. The tool temperature was set at 130°C and monitored by two thermocouples. The tool was spray-coated with a release agent (Chemlease® PMR EZ, Chem-Trend L.P. Howell, US) to facilitate demolding after processing. After processing, plates were cooled down in free air up to room temperature. In a previous study [14], the authors reported tensile and flexural moduli of 58 GPa and 50 GPa, respectively, with ultimate strengths of 446 MPa and 830 MPa.

Single-lap joints were fabricated following the recommendations outlined in ASTM Standard D5868 (“Lap Shear Adhesion for Fiber Reinforced Plastics”). Composite panels were machined into $100 \times 25 \times 2.5 \text{ mm}$ flat coupons and used for adhesive bonding. Additionally, $25 \times 25 \text{ mm}$ alignment tabs were prepared similarly.

The adhesive chosen for structural bonding is a toughened structural epoxy Hysol 9466 (Henkel-Loctite) which exhibits exceptional resistance to both peeling and shear forces. It also offers excellent resistance to a wide range of chemicals and solvents, while providing strong dielectric insulating properties. This makes it particularly suitable for demanding environments where both mechanical strength and chemical resistance are essential.

Surface Preparation Methods

The bonding process began with manual abrasion, which was used as a standalone treatment to establish baseline surface conditions on the composite adherends. This step involved light sanding of both adherent surfaces with 240-grit sandpaper, applied in a cross-hatch pattern to ensure uniform abrasion. The goal was to remove surface contaminants, oils, and residues that could reduce adhesion at the adhesive/substrate interface. Manual abrasion also aims to increase surface roughness and surface area, potentially promoting micro-interlocking between the adhesive and the composite material [4]. As a result, the roughened surface should provide a more favorable environment for adhesive bonding, thereby improving bond strength.

Following the abrasion, the treated surfaces were thoroughly cleaned with isopropyl alcohol and wiped with a lint-free cloth to remove any residual dust or particles. This step ensured that no contaminants remained to compromise the bond during the subsequent adhesive application.

An ultrashort pulsed laser was used to perform the alternative surface preparation process. A schematic of the corresponding experimental apparatus is shown in Figure 1a. The laser source is an Ekspla Atlantic 50, characterized by a pulse duration of about 10 ps. The chosen wavelength was 355 nm, as it should prevent or minimize damage to the reinforcing carbon fibers. The repetition rate was chosen equal to 300 kHz to deliver the maximum energy per pulse allowed by the laser source. Furthermore, the laser system was equipped with a Raylase Superscan V galvanometric scanning head to precisely control and direct the laser to the target, while an F-theta type lens ensured a beam diameter of about $10 \mu\text{m}$ at $1/e^2$ intensity.

The idea is to operate a uniform surface treatment, to ablate the material layer where the release agent has penetrated. Therefore, a rectangular scanning pattern with an area of $14 \times 28 \text{ mm}^2$ was

selected to cover the target bonding area. The pattern consists of parallel lines, scanned at 1000 mm/s, and oriented at 45° to ensure there is no preferential treatment of either horizontal or vertical fibers, as shown in Figure 1b and Figure 1c.

The laser processing parameters were varied as follows: power attenuation ranging from 12% to 35%, (corresponding to 4,70 W at 100%), scan step from 3 μm to 5 μm (with overlap exceeding 50%), and number of passes from 2 to 35.

The final processing parameters, which represented a compromise between preserving the as-received material and achieving complete matrix removal were: 300 kHz of repetition rate, 4 μm line spacing, 1000 mm/s of scan speed, 7 passes, 0.68 W of power, corresponding at 2.26 μJ energy per pulse and 2.88 J/cm² fluence. Eight samples were treated to ensure at least four pairs of adherends for subsequent mechanical testing.

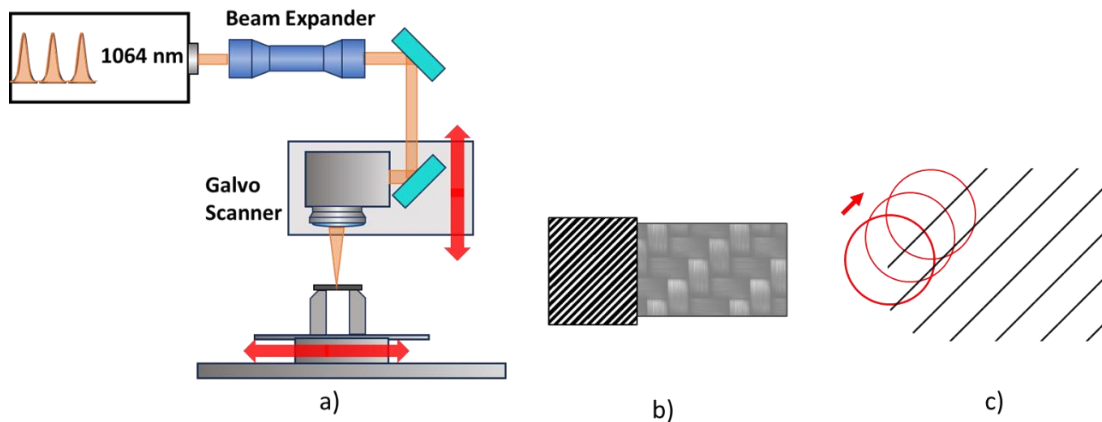


Figure 1. a) Laser system; b,c) CFRP laser treatment scheme: 45° parallel lines.

Characterization of surface morphology and chemistry

To select laser parameters, the laser-treated specimens were first observed through an optical microscope Nikon Eclipse LV100ND with five physical objectives from 5x to 100x. The microscope stage can be adjusted in the z direction with relative motions of 1 μm. This was utilized to assess the laser treatment depth: the treated region's bottom surface and the untreated material's top surface were focused in two different z positions, they were noted, and by measuring the difference the depth is derived.

Then, a scanning electron microscope Nova NanoSEM 450 (Fei Company) was used to investigate the surface morphology of the specimens at different magnifications, while the surface composition was analyzed by EDS analysis (X-EDS Oxford INCA-350).

Point spectra and elemental maps were acquired after 120 seconds of analysis in both the matrix and fiber regions for untreated, sanded, and laser-treated specimens. The percentage of silicon versus carbon only (base material of the matrix and fiber) was evaluated, having a clearer comparison of the decrease of Si. A low-vacuum solid-state BSED (GDA) sensor was used.

Single-Lap Joint manufacturing and mechanical testing

Following completion of surface treatments, eight single-lap adhesive joints were manufactured for subsequent mechanical testing (Figure 2). The adhesive was uniformly applied to the bonding area of the bottom adherend. To ensure the desired 0.25 mm bondline thickness, two equally spaced calibrated nylon wires were fixed to the bottom adherend within the bonding area and along the loading direction, i.e. the x - direction in Figure 2, acting as spacers. Once the adhesive had

been applied, the top adherend was put in place, ensuring proper alignment of the joint through a purposely developed fixture. The same procedure was followed to bond the alignment tabs.

The joint was then clamped to ensure a consistent pressure throughout the curing process, which consisted of three hours at 40°C to ensure complete curing and optimal mechanical properties, as suggested in the manufacturer's technical data sheet [16].

After the curing, the joints underwent a thorough inspection to verify the integrity of the bond. This included visual checks for uniformity and measurement of the bondline thickness. Post-curing single-lap joints inspection revealed a bondline thickness of about 400 μm . Figure 2 shows a sketch of the single-lap joint and ensuing dimensions.

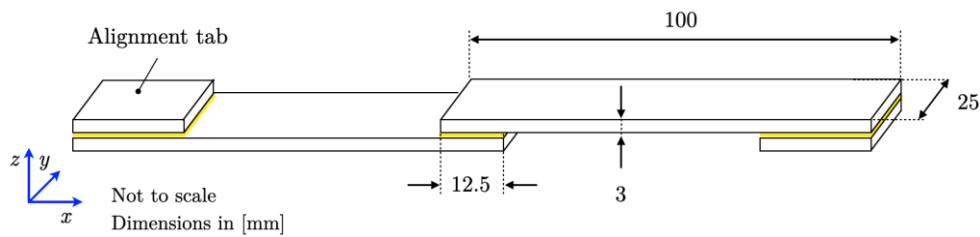


Figure 2. Schematic of the single lap adhesive joint specimen.

Tensile tests were performed on a Galdabini Quasar 25, an electromechanical testing machine equipped with a 25 kN loading cell and manual clamping fixtures. The specimens were carefully clamped on the area of the alignment tabs. The test applied a preload of 200 N followed by a constant tensile speed of 1 mm/min, up to complete failure of the joint: the proprietary software that controls the machine allowed to register the force-displacement curves.

Results and Discussion

SEM/EDS morphological and chemical results

The as-produced, sanded, and laser-treated surfaces were analyzed using scanning electron microscopy (SEM) and Energy Dispersive X-ray Spectroscopy (EDS) elemental analysis to qualitatively identify the release agent (i.e., silicon contamination) and to quantify its percentage.

The results are presented in Figure 3, where silicon contamination is highlighted in pink, and the carbon content is indicated in black.

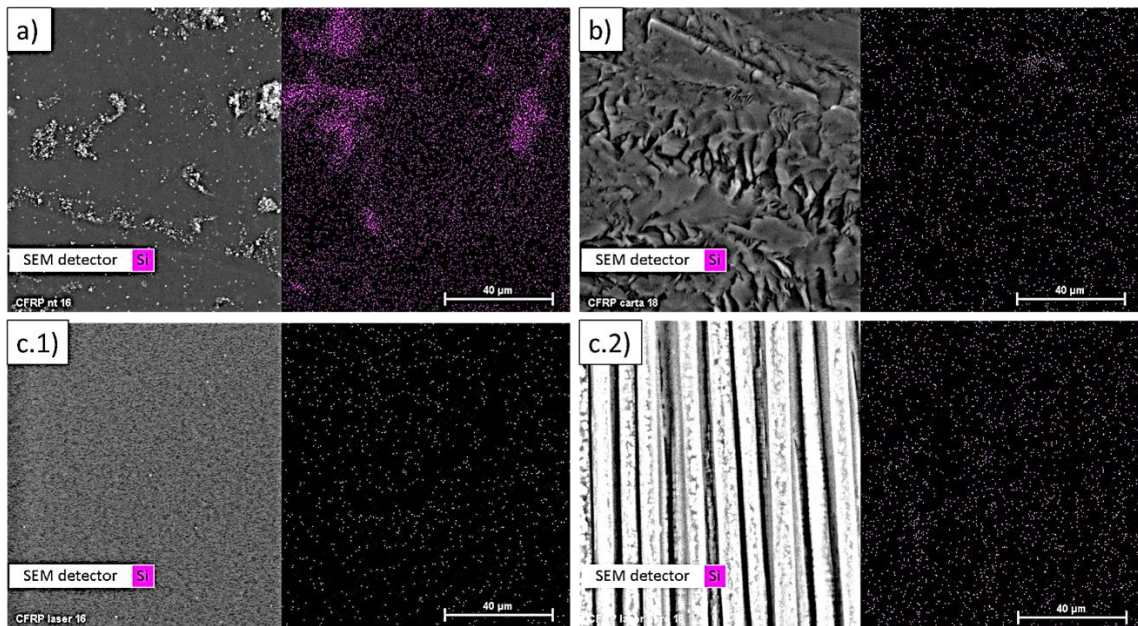


Figure 3. SEM/EDS of a) untreated, b) sanded material, and laser-treated material: c.1) matrix, c.2) fibers.

The silicon percentage decreased from the untreated (Figure 3a) to the sanded (Figure 3b) and laser-treated (Figure 3c.1 and c.2) materials. For the laser-treated surfaces, the release agent remains in a few evenly distributed spots, likely still embedded within the composite thickness. Additionally, Figure 3b shows that the morphology of the sanded material is irregular, with uneven removal of the release agent, which appears to be thicker in some areas, but anyway is substantially decreased.

As determined from both point spectrum and elemental mapping, the elemental composition indicates a significant reduction in silicon content for both the sanded and laser-treated samples. According to the point spectrum data presented in Table 1, the silicon percentage in the laser-treated sample (at the matrix level) is approximately half that of the sanded sample. Moreover, in regions where the fiber is closer to the surface (indicated as "Fiber"), the silicon content is further reduced.

Table 1. EDS point elemental analysis.

Specimen	%C	%Si
As-is	91.53	8.47
Sanded (manual abrasion)	99.79	0.21
UV-laser (matrix)	99.91	0.09
UV-laser (fiber)	99.98	0.02

While the SEM analysis provides high-resolution details at the microscale, optical microscope images can offer a macroscopic view of the material surface, which allows to observe larger-scale effects of the laser treatment. As such, optical microscope images are reported in Figure 4 to illustrate the effect of laser treatment on the release agent stains.

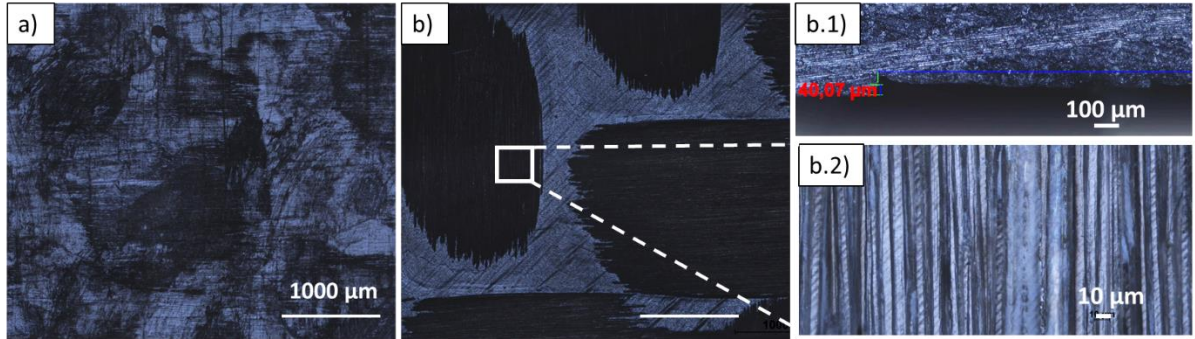


Figure 4. Optical microscope image of (a) untreated and (b) laser-treated sample: (b.1) cross section, and (b.2) fibers.

In comparison to the untreated material (Figure 4a), the laser treatment (Figure 4b) effectively removes most of the visible release agent. This removal process involves ablating the matrix material to a depth of up to 40 μm (Figure 4b1). Furthermore, Figure 4b.2 shows that the fibers remain unaffected by the laser treatment, as they appear transparent beneath the layer of matrix, with processing marks clearly visible.

By increasing either the number of laser passes or the laser power, the matrix can be completely removed, exposing the fibers without causing damage. However, this represents the upper limit of the processing parameters, which remains to be explored in subsequent works.

Mechanical tensile test results

The mechanical test results are presented in Figure 5, which illustrates the load-displacement curves obtained from the tensile tests. The single-lap joint tests exhibit a characteristic load-displacement response, initially displaying linear behaviour, followed by a distinct "knee" in the curve (typically in the range from 2 kN to 3 kN), where the slope changes. After this transition, the curve continues with a nearly constant slope until failure occurs. Notably, sanded and laser-treated joints exhibit a similar bilinear response, and the post failure inspection of the joint indicates that the transition is not related to damage or fracture of the adherends but rather it likely reflects the adhesive behaviour under stress, i.e. the occurrence of inelastic deformations.

The laser-treated joints generally exhibit a higher displacement at failure compared to the sanded specimens, which implies enhanced ability by the adhesive to absorb energy prior to failure. It is surmised that the improved displacement at failure is likely due to the more effective surface preparation provided by the laser treatment, which facilitates the removal of release agents and enhances adhesion at the adhesive-substrate interface.

The load-displacement plots clearly show that, in all cases, the laser-treated specimens exhibit a higher maximum load compared to the sanded specimens, with the sole exception of a single sanded specimen that reached a maximum load comparable to that of the laser-treated samples. The shear strength of both sets of specimens was calculated by dividing the maximum load by the bonded area. The average shear strengths were found to be 14.5 ± 1.7 MPa for the sanded joints and 16.8 ± 1.0 MPa for the laser-treated joints, representing an approximate 14% increase in shear strength for the laser-treated specimens.

Variability in the testing of manual abrasion specimens is intrinsic to the manual process, whereas in laser processing it is mostly found in one pair of specimens that deviates from the others. This may be due to the base surface not always being regular, which locally produced variability in laser processing. In any case, the latter is approximately 5%, compared to manual abrasion, in which variability exceeds 10%.

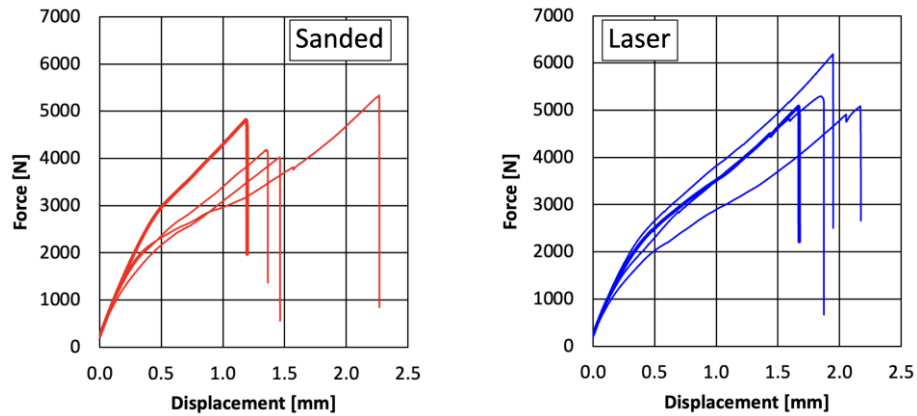


Figure 5. Load versus Displacement for Sanded (red) and Laser Treated samples (blue)

Finally, the fracture surfaces of the specimens were visually examined to identify the primary failure mechanisms, and the results are shown in **Error! Reference source not found.**. In the case of the laser-treated samples, the fracture surface was notably characterized by the presence of adhesive residues on both sides of the joint, suggesting that the fracture propagated through the adhesive layer, indicative of cohesive failure within the adhesive itself. **Error! Reference source not found.** highlights specific locations of such transitions, where the arrows point to regions that suggest direct anchoring of the adhesive to the carbon fibers. Furthermore, visual inspection also suggests that at such location carbon fibers were likely stripped from the CFRP adherent during failure. It is worth noting that this additional dissipation mechanism, when carefully controlled, could potentially enhance the overall performance of the adhesive bond [15].

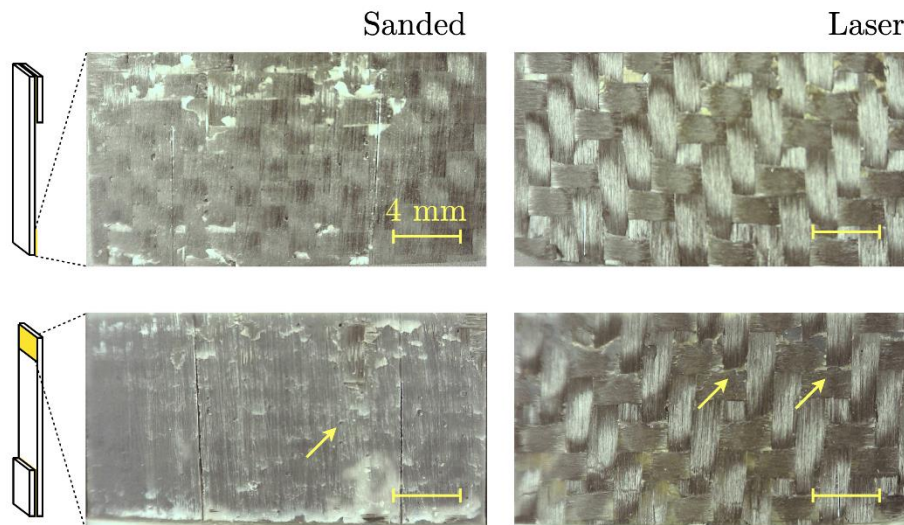


Figure 6. Fracture surface of sanded and laser-treated specimens.

In contrast, the fracture surfaces of the sanded specimens exhibited a more pronounced interfacial failure mode, with fracture occurring primarily at the adhesive-substrate interface. Closer inspection revealed localized surface whitening in certain areas. Surface whitening is typically associated with mechanical deformation and densification of the adhesive at the interface, suggesting effective adhesion in these regions. Additionally, the sanded specimens showed a more

significant formation of air voids at the interface, which may indicate weaker adhesion in specific areas. An example of such voids is marked by arrows in **Error! Reference source not found.** Although air voids may also be present in the laser-treated joints, their presence is less evident in the available images.

Conclusions

The present study evaluated the effect of surface preparation on the adhesive bonding of carbon fiber-reinforced prepreg compression molding laminate specimens. The quality of adhesive joints is highly dependent on the surface morphology, topography, and composition of the adherend-adhesive interface. For molded composites, the presence of release agents, which are often absorbed into the outermost layer of the material, significantly impacts adhesion and weakens adhesive joint properties.

In this context, the current study compared the effects of standard mechanical abrasion (manual sanding) and ultrashort UV laser processing in terms of their ability to remove contaminants and generate surfaces that enhance adhesion and improve the mechanical strength of the joints. The impact of surface preparation was investigated through SEM-EDS analysis and mechanical testing of epoxy-bonded single-lap joints.

The results demonstrate that the selected UV picosecond laser treatment can remove the matrix material while leaving the carbon fibers largely undamaged. EDS analysis in areas where the fibers were more exposed - due to a deeper ablation of the matrix - showed a significant reduction in silicon content, indicating more effective removal of the release agent. Preliminary tensile tests revealed a 14% increase in the average shear strength of laser-treated joints compared to sanded specimens. This improvement is attributed to a more homogeneous removal of the release agent, as confirmed by SEM/EDS analysis. Additionally, visual inspection of the fracture surfaces revealed a shift in failure mode from adhesive failure to cohesive failure for the laser-treated samples.

It is important to note that the current laser process has not yet been fully optimized, which likely contributes to the observed variability in the mechanical test results. Consequently, these findings should be regarded as preliminary. While the observed improvements in shear strength and the shift in failure modes are promising, further research is required to optimize the laser treatment parameters and fully evaluate its potential.

Acknowledgements

The authors wish to thank Ing. Simone Zanetti at Henkel Italia S.r.l., Milano, Italy, for supplying the epoxy adhesive employed in this research.

Fundings

This work was supported by Emilia-Romagna regional project PR FESR 2021-2027, 1, 1.1.2, "SAFER", CUP E17G22001630003.

References

- [1] C. Leone, A. Paoletti, P. Babu Yanala, F. Lambiase, Improving bonding strength of aluminium-PEEK hybrid metal-polymer joints by two-step laser surface treatment, *Optics & Laser Technology* 170 (2024) 110304. <https://doi.org/10.1016/j.optlastec.2023.110304>.
- [2] A. Yudhanto, M. Alfano, G. Lubineau, Surface preparation strategies in secondary bonded thermoset-based composite materials: A review, *Composites Part A: Applied Science and Manufacturing* 147 (2021) 106443. <https://doi.org/10.1016/j.compositesa.2021.106443>.
- [3] N. Karthikeyan, J. Naveen, Progress in adhesive-bonded composite joints: A comprehensive review, *Journal of Reinforced Plastics and Composites* (2024) 07316844241248236. <https://doi.org/10.1177/07316844241248236>.

- [4] C. Morano, R. Tao, M. Alfano, G. Lubineau, Effect of Mechanical Pretreatments on Damage Mechanisms and Fracture Toughness in CFRP/Epoxy Joints, *Materials* 14 (2021) 1512. <https://doi.org/10.3390/ma14061512>.
- [5] A. Zhang, H. Jiang, Y. Li, R. Hu, Y. Ren, S. Jiang, Effects of surface micro-texturing laser-etching on adhesive property and failure behaviors of basalt fiber composite single-lap-joint, *International Journal of Adhesion and Adhesives* 135 (2024) 103831. <https://doi.org/10.1016/j.ijadhadh.2024.103831>.
- [6] S.P. Sharma, R. Vilar, Femtosecond laser micromachining of carbon fiber-reinforced epoxy matrix composites, *Journal of Manufacturing Processes* 84 (2022) 1568–1579. <https://doi.org/10.1016/j.jmapro.2022.10.009>.
- [7] R.I. Ledesma, F.L. Palmieri, Y. Lin, M.A. Belcher, D.R. Ferriell, S.K. Thomas, J.W. Connell, Picosecond laser surface treatment and analysis of thermoplastic composites for structural adhesive bonding, *Composites Part B: Engineering* 191 (2020) 107939. <https://doi.org/10.1016/j.compositesb.2020.107939>.
- [8] L. Sorrentino, S. Marfia, G. Parodo, E. Sacco, Laser treatment surface: An innovative method to increase the adhesive bonding of ENF joints in CFRP, *Composite Structures* 233 (2020) 111638. <https://doi.org/10.1016/j.compstruct.2019.111638>.
- [9] Y. Yuan, X. Guo, H. He, K. Zhang, W. Han, Rapid surface patterning to strengthen adhesive bonding of carbon fiber reinforced polymer by spatial shaping femtosecond laser, *Optics & Laser Technology* 180 (2025) 111562. <https://doi.org/10.1016/j.optlastec.2024.111562>.
- [10] A.A. Andarabi, K. Shelesh-Nezhad, T.N. Chakherlou, The effect of laser surface structuring patterns on the interfacial resistance of aluminum joints bonded with epoxy adhesive, *International Journal of Adhesion and Adhesives* 114 (2022) 103101. <https://doi.org/10.1016/j.ijadhadh.2022.103101>.
- [11] R. Tao, X. Li, A. Yudhanto, M. Alfano, G. Lubineau, Laser-based interfacial patterning enables toughening of CFRP/epoxy joints through bridging of adhesive ligaments, *Composites Part A: Applied Science and Manufacturing* 139 (2020) 106094. <https://doi.org/10.1016/j.compositesa.2020.106094>.
- [12] C. Morano, R. Tao, A. Wagih, M. Alfano, G. Lubineau, Toughening effect in adhesive joints comprising a CFRP laminate and a corrugated lightweight aluminum alloy, *Materials Today Communications* 32 (2022) 104103. <https://doi.org/10.1016/j.mtcomm.2022.104103>.
- [13] L. Raimondi, T.M. Brugo, A. Zucchelli, Fiber misalignment analysis in PCM-UD composite materials by Full Field Nodal Method, *Composites Part C: Open Access* 5 (2021) 100151. <https://doi.org/10.1016/j.jcomc.2021.100151>.
- [14] L. Raimondi, Effects of UD and twill reinforcements in hybrid sheet molding compound laminates, in: 2024: pp. 523–529. <https://doi.org/10.21741/9781644903131-58>.
- [15] G. Lubineau, M. Alfano, R. Tao, A. Wagih, A. Yudhanto, X. Li, K. Almuhammadi, M. Hashem, P. Hu, H.A. Mahmoud, F. Oz, Harnessing Extrinsic Dissipation to Enhance the Toughness of Composites and Composite Joints: A State-of-the-Art Review of Recent Advances, *Advanced Materials* 36 (2024) 2407132. <https://doi.org/10.1002/adma.202407132>.
- [16] www.henkel-adhesives.com/it/it/prodotto/structural-adhesives/loctite_ea_94661.html